Biomaterials Science

Single-tailed Heterocyclic Carboxamide Lipids for Macrophage Immune-Modulation

Journal:	*Biomaterials Science*
Manuscript ID	BM-COM-11-2022-001804.R1
Article Type:	Communication
Date Submitted by the Author:	05-Mar-2023
Complete List of Authors:	Mei, Kuo-Ching; State University of New York at Binghamton, School of Pharmacy and Pharmaceutical Sciences; UNC Eshelman School of Pharmacy Stiepel, Rebeca; UNC Eshelman School of Pharmacy Bonacquisti, Emily; UNC Eshelman School of Pharmacy Jasiewicz, Natalie; UNC Eshelman School of Pharmacy Chaudhari, Ameya; UNC Eshelman School of Pharmacy Tiwade, Palas; UNC Eshelman School of Pharmacy Bachelder, Eric; University of North Carolina, Division of Molecular Pharmaceutics Ainslie, Kristy; University of North Carolina at Chapel Hill , Pharmacy Fenton, Owen; UNC Eshelman School of Pharmacy Nguyen, Juliane; University of North Carolina at Chapel Hill,

COMMUNICATION

Single-tailed Heterocyclic Carboxamide Lipids for Macrophage Immune-Modulation

Received 00th January 20xx,
Accepted 00th January 20xx

DOI: 10.1039/x0xx00000x

Kuo-Ching Mei,*[a, b] Rebeca T. Stiepel,[a] Emily Bonacquisti,[a] Natalie E. Jasiewicz,[a] Ameya Pravin Chaudhari,[a] Palas B. Tiwade,[a] Eric M. Bachelder,[a] Kristy M. Ainslie,[a] Owen S. Fenton,[a] and Juliane Nguyen*[a]

The discovery of new immune-modulating biomaterials is of significant value to immuno-engineering and therapy development. Here, we discovered that single-tailed heterocyclic carboxamide lipids preferentially modulated macrophages – but not dendritic cells - by interfering with sphingosine-1-phosphate-related pathways, consequently increasing interferon alpha expression. We further performed extensive downstream correlation analysis and determined key factors in physicochemical properties likely to modulate pro-inflammatory and anti-inflammatory immune responses. These properties will be useful for the rational design of the next generation of cell type-specific immune-modulating lipids.

Immuno-engineering is a rapidly progressing field driven by the discovery of immune-modulating biomaterials.[1] Lipids have attracted particular attention as immune-engineering biomaterials due to their ability to self-assemble into drug and gene-delivering carriers and their recognized but complex interplay with the immune system.[2] For example, cationic lipids, when formulated into liposomes, can induce the upregulation of co-stimulatory membrane proteins CD80 and CD86 on dendritic cells.[3] The sphingolipid/ceramide family of amide-containing lipids have also been found to stimulate dendritic cells, consequently promoting effector T cell responses.[4] Conversely, bio-inert lipids and lipid-drug conjugates have been used extensively to formulate liposomes for drug delivery and modulate the immune microenvironment in cancer.[5-7] Ionizable cationic lipids capable of delivering mRNAs in the form of lipid nanoparticles (LNPs), have led to new avenues for engineered immunity, as demonstrated by the COVID vaccines.[8] Upon delivery of mRNA-based LNP vaccines to dendritic cells, heterocyclic (cationic) ionizable lipids have been shown to activate the stimulator of the interferon genes (STING) pathway triggering type I interferons (*e.g.,* IFN-α), thereby enhancing anti-tumor immunity.[9] On the other hand, a single-tailed lipid-like sphingosine-1-phosphate (S1P) receptor modulator, fingolimod (Gilenya®), has been approved for clinical use as an effective immune modulator for patients with multiple sclerosis (MS),[10] inspiring further development of lipid-like immune-modulating biomaterials. Interestingly, S1P lysate is known to activate IκB kinase ε (IKKε), promoting type I IFN–mediated innate immune responses.[11] Intrigued by these findings, we designed a focused library of heterocyclic carboxamide lipids with combined features of interest for immune stimulation, namely amine/amide and heterocyclic rings (pyrrolidine, morpholine, piperazine), as shown in **Scheme 1**. We also incorporated an alkyne (propargyl) side chain to enable future derivatizations of these carboxamide lipid scaffolds.

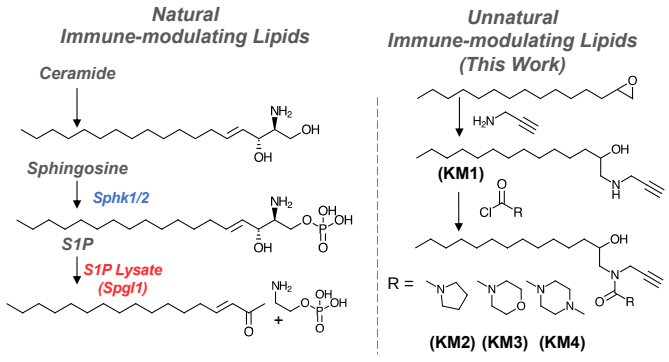

Scheme 1. Overall synthesis of the immune-modulating heterocyclic carboxamide lipids for interfering with S1P lipid signalling pathway.

We hypothesized that by combining immune-stimulating features, we would observe new immune-modulating interactions interfacing with the S1P-related signaling pathway.

[a] Division of Pharmacoengineering and Molecular Engineering, UNC Eshelman School of Pharmacy, University of North Carolina at Chapel Hill, Chapel Hill NC, 29599.
[b] Department of Pharmaceutical Sciences, School of Pharmacy and Pharmaceutical Sciences, State University of New York at Binghamton, Binghamton NY, 13790.

* Correspondence to julianen@email.unc.edu and kmei@binghamton.edu
Electronic Supplementary Information (ESI) available: [details of any supplementary information available should be included here]. See DOI: 10.1039/x0xx00000x

As illustrated in **Scheme 1**, we started by synthesizing heterocyclic carboxamide lipids in two steps: (i) Nucleophilic epoxy ring-opening of 1,2-epoxytetradecane *via* propargylamine to produce the ionizable propargyl lipid **KM1** as (ii) reactions between acid chlorides and amines to produce heterocyclic carboxamide lipids **KM2** (yield = 83%), **KM3** (yield = 74%) and Lipid **KM4** (yield = 33%) The synthesis methods, ^{1}H NMR, ^{1}H-^{1}H COSY-NMR, ^{13}C NMR, and ESI-MS spectra of the lipids can be found in the online Supporting Information (**Figures S1 – S16**). All lipids were screened for endotoxin after purification using the Pierce™ Chromogenic Endotoxin Quant kit (ThermoFisher Scientific). All lipid samples had undetectable levels of endotoxin (< 0.1 EU/mg, **Figure S17**).

To test our hypothesis that our new heterocyclic carboxamide lipids would mediate lipid-enabled immuno-modulatory effects, we focused on two antigen-presenting cells: murine DC2.4 dendritic cells (Sigma) and murine RAW 264.7/NF-kB Renilla luciferase reporter macrophage cell line (Crownbio). Cells were seeded in 24-well plates (1 x 10^5 cells/well) overnight and incubated with lipids (5 μM) for 6 hours, and all treated cells had >85% viability under the experimental conditions tested (**Figure S18-19**). Single-tailed lysophosphatidylcholine (LysoPC) was used as the control lipid. Quantitative reverse transcription-polymerase chain reaction (qRT-PCR) was used to evaluate cellular responses to the lipids. We investigated genes related to possible immune responses of interest, including NF-κB (signaling via toll-like receptors),[12] sphingolipid-related signaling pathways, e.*g.,* Rho-associated protein kinase (*Rock1*), sphingosine kinase 2 (*Sphk2*), and sphingosine-1-phosphate lyase 1 (*Spgl1*),[13] immune checkpoints downstream of interferon receptor signaling pathways, *e.g.,* indoleamine-pyrrole 2,3-dioxygenase (IDO1) and programmed death-ligand 1 (PD-L1, encoded by *CD274*),[14, 15] the type I interferons such as interferon alpha (*Ifna1*),[9, 16] and inducible nitric oxide synthase (iNOS, encoded by Nos2a), representing inflammatory responses in macrophages and mature dendritic cells.[17] In brief, after 6 h incubation with the lipids, macrophages and dendritic cells were gently washed three times with phosphate-buffered saline three times before being lysed for RNA extraction using the RNeasy mini kit (Qiagen). cDNA was synthesized from the isolated RNA using the iScript™ cDNA synthesis kit (Bio-Rad). Forward and reverse RT-PCR primers (see **Table S1** for primer sequences) of Gapdh (housekeeping gene), *Nfkb, Rock1, Sphk2, Spgl1, Ido1, Cd274* (PD-L1), *Ifna1*, and *Nos2a* (iNOS) were mixed with iTaq Universal SYBR Green Supermix (Bio-Rad) and amplified/detected in an RT-PCR system (QuantStudio 3™). The CT (cycle threshold) values were analyzed using Design and Analysis Software v1.5.2. Fold changes in gene expression changes were evaluated using delta-delta CT analysis normalizing to *Gapdh*. The results expressed as fold changes in gene expression are shown in **Figure 1**. Interestingly, all lipids failed to induce significant changes in DC2.4 dendritic cells. Instead, preferential immune-modulating responses were observed in RAW264.7 macrophages (**Figure 1**). In macrophages, there was generally greater sphingosine-1-phosphate lyase *(Spgl1)* expression in groups treated with the KM-lipid series. S1P lyase, by degrading S1P, is a key regulator of the S1P signaling pathway, known to promote type I IFN–mediated innate immune responses.[11, 18, 19] Consistent with the literature, we found the highest upregulation of IFN-α and *Spgl1* when induced by heterocyclic carboxamide lipids **KM2**, **KM3**, and **KM4**, but not non-heterocyclic lipids **KM1** and LysoPC.

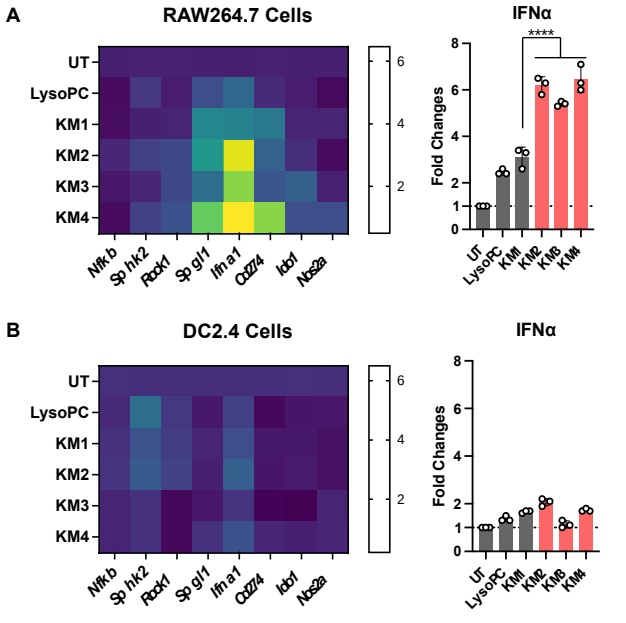

Figure 1. Differential Immune-modulation of macrophages compared to dendritic cells by heterocyclic carboxamide lipids. Fold changes in gene expression in RAW264.7 macrophages and DC2.4 dendritic cells after incubating with control and heterocyclic carboxamide lipids for 6 h. Heterocyclic carboxamide lipids induced the highest gene expression of IFN-α (*Ifna1*) in DC2.4 cells compared with lipids without heterocyclic carboxamide rings. PD-L1(Cd274) and Spgl1 were also expressed at higher levels in DC2.4 cells. Such changes in gene expression were preferentially induced in RAW264.7 macrophages compared to DC2.4 dendritic cells. Statistics: **** $p < 0.0001$, $n = 3$, one-way ANOVA calculated using GraphPad Prism software.

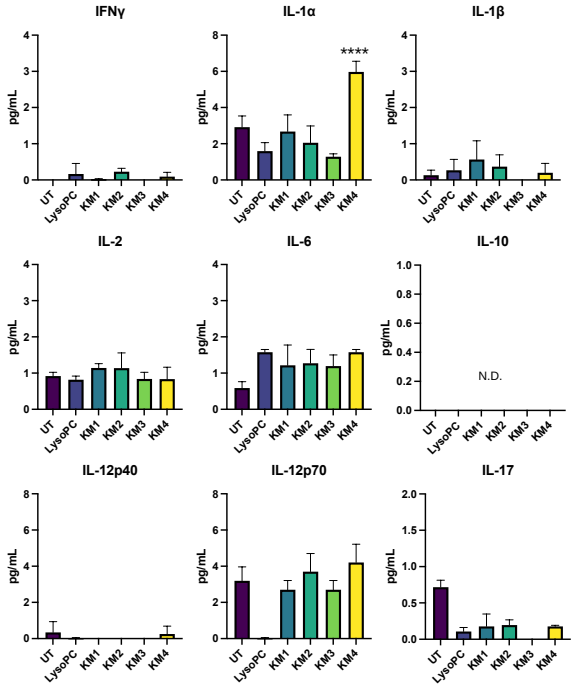

Figure 2. Cytokine release profiles of RAW264.7 Cells after treatment with heterocyclic carboxamide lipids. Cell culture supernatants were taken at 6 h time point after lipid treatments.

Heterocyclic carboxamide Lipids **KM4** also induced the highest expression of PD-L1 (*Cd274*; **Figure 1**), consistent with the literature, as IFN-α has been shown to upregulate the immunosuppressive PD-L1.[20] This PD-L1 upregulation was decoupled from *Ido1*, suggesting that the immune regulation was mainly through IFN-α rather than IFN-γ signaling.[5, 21, 22] The cytokine release studies were performed to assess the effectiveness of IFN-α stimulation by analyzing the cell culture supernatants at 6 h post-incubation (**Figure 2**). It is worth noting that while IFN-α stimulation has potential applications in immunotherapy,[23] its stimulation in human/murine macrophages also increases the oxidized low-density lipoprotein (ox-LDL) induced forma cell formation, which is a key first step in atherosclerosis.[24, 25] This effect involves S1PR2/Rho/ROCK pathway and is known to be diminished in mice lacking S1PR2 and apoE ($S1pr2^{-/-}Apoe^{-/-}$).[26, 27] Our results further indicate a strong correlation between *Rock1* and *Ifna1* expression levels (R^2 = 0.9265), suggesting potential interferences by the KM lipids *via* the S1PR2 pathway (**Figure S20-22**).

To better understand the physicochemical properties of these heterocyclic carboxamide lipids were analyzed using Marvin Sketch (ChemAxon). Each lipid was categorized by 27

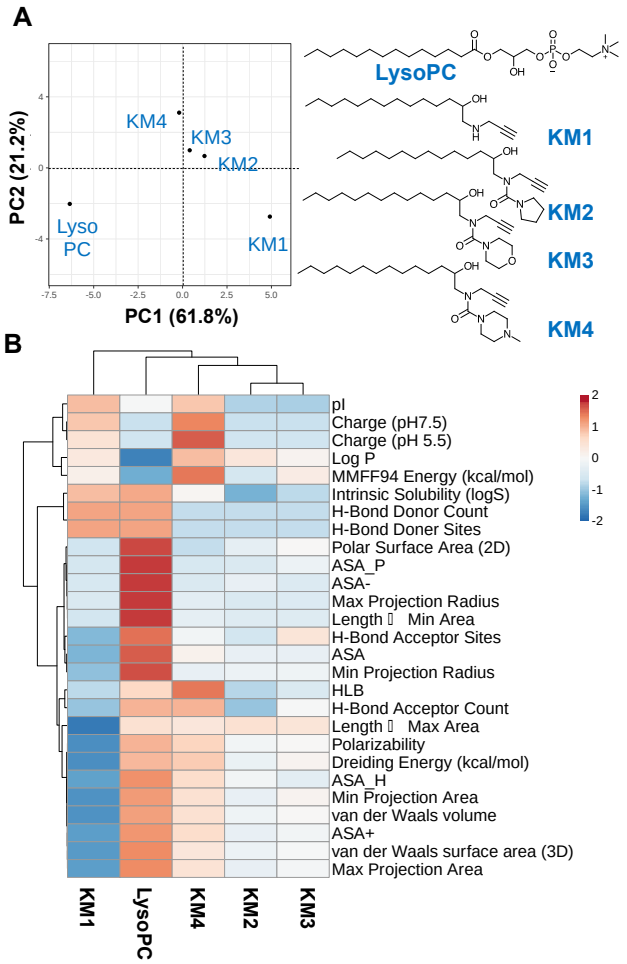

Figure 3. Principal component analysis (PCA) of the physicochemical properties of heterocyclic carboxamide lipids. A) PCA score plot of the lipids. Data points are separated on the principal components based on their differences in physicochemical properties. B) Heatmap of the physicochemical properties of the lipids clustering based on their similarity in properties.

A

	PC1
Log P	0.19
MMFF94 Energy (kcal/mol)	0.12
Charge (pH7.5)	0.11
Charge (pH 5.5)	0.08
pI	0.04
H-Bond Donor Count	-0.04
H-Bond Doner Sites	-0.04
Intrinsic Solubility (logS)	-0.06
HLB	-0.14
Length ⊥ Max Area	-0.17
H-Bond Acceptor Count	-0.19
Dreiding Energy (kcal/mol)	-0.21
Polar Surface Area (2D)	-0.22
Polarizability	-0.22
ASA-	-0.22
Max Projection Radius	-0.22
ASA_P	-0.22
Length ⊥ Min Area	-0.23
van der Walls volume	-0.23
Min Projection Area	-0.23
ASA_H	-0.23
ASA+	-0.23
H-Bond Acceptor Sites	-0.23
van der Waals surface area (3D)	-0.24
Max Projection Area	-0.24
Min Projection Radius	-0.24
ASA	-0.24

	PC2
MMFF94 Energy (kcal/mol)	0.28
Length ⊥ Max Area	0.26
Log P	0.25
Dreiding Energy (kcal/mol)	0.21
Polarizability	0.19
HLB	0.19
Charge (pH 5.5)	0.17
van der Walls volume	0.15
Min Projection Area	0.15
H-Bond Acceptor Count	0.14
ASA+	0.13
ASA_H	0.11
van der Waals surface area (3D)	0.11
Max Projection Area	0.11
Charge (pH7.5)	0.09
ASA	0.00
H-Bond Acceptor Sites	-0.01
pI	-0.06
Min Projection Radius	-0.07
Length ⊥ Min Area	-0.15
Max Projection Radius	-0.17
Polar Surface Area (2D)	-0.18
ASA_P	-0.18
ASA-	-0.19
Intrinsic Solubility (logS)	-0.26
H-Bond Donor Count	-0.38
H-Bond Doner Sites	-0.38

B

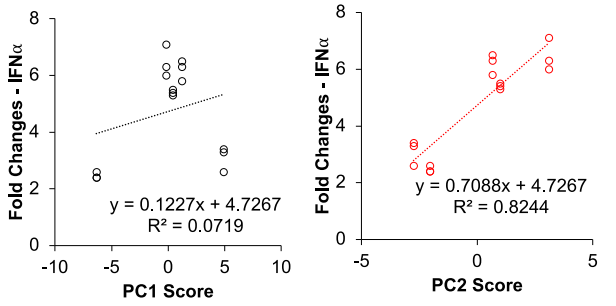

Figure 4. The loading of principal component analysis loading for of IFNα expression levels. A) PCA loadings for PC1 and PC2 scores are listed and sorted from positive to negative values. Physicochemical properties with positive or negative PCA loadings contribute to the positive or negative PCA scores as shown in Figure 2A. B) Correlation analysis of fold changes in IFNα expression in RAW264.7 cells as a function of PC1 or PC2 scores indicated that PC2 scores are the major driver positively correlated with IFNα expression, *i.e.,* the physicochemical properties that have positive PCA loadings contribute to increased IFNα expression.

physicochemical properties, *e.g.,* physical geometry, polarizability, hydrogen bond donor/acceptor sites, LogP (partition coefficient), LogS (intrinsic solubility), hydrophilic-lipophilic balance (HLB) values, isometric point (pI), charges at pH 7.4/5.5, van der Waals surface area, and their solvent accessible surface area (ASA) (**Table S2**). Principal component analysis (PCA) was then applied to reduce and project the 27 factors/dimensional data into an artificial two-dimensional coordinate space as principal component 1 (PC1) and principal component 2 (PC2), which accounted for 61.8% and 21.2% of the variance caused by these lipids, respectively. The final result was visualized as a PCA score plot and clustered as a heatmap using ClustVis as shown in **Figure 3**.[28] In the PCA score plot (**Figure 3A**), data points were spatially separated based on their differences in physicochemical properties, especially distinct separation of LysoPC and the heterocyclic carboxamide lipids. Furthermore, the heterocyclic carboxamide lipids showed roughly linear sequential changes reflecting the changes in the heterocyclic rings. The overall differences in physicochemical properties were visualized as a heat map, with unsupervised clustering visualizing the similarities between the lipids (**Figure**

3B). The details of the PC1 and PC2 loadings, listed and sorted from positive to negative values, are shown in **Figure 4A**, where physicochemical properties with positive or negative PCA loadings contribute to the positive or negative spatial separation in the PCA score plot (**Figure 3A**). Correlation analysis of fold changes in IFN-α expression as a function of PC1 or PC2 scores indicated that PC2 scores – not PC1 scores - were the major driver positively correlated with IFNα expression. In other words, the physicochemical properties with positive PC2 loadings contribute to increased PC2 scores and IFNα expression (**Figure 4B, Table S2-S4**).

Based on the preliminary findings from the PCA studies, we performed a linear correlation analysis using fold changes in S1P lysate (*Spgl1*, **Figures S23-S26**) and IFN-α (*Ifna*) expression as a function of each physicochemical property. The full result is shown in **Figures S27-S29.** Based on the slope of the linear regression and the R^2 values of the correlations, the summarized and sorted results are shown in **Figure 4A**. Factors with the strongest positive correlation with IFNα expression levels included the partition coefficient (LogP) and Merck molecular force field (MMFF94) energy.[29] Higher LogP (meaning more lipophilic) and MMFF94 energy positively correlated with higher IFN-α expression. Factors such as lipid charges at pH 7.5, van der Waals surface area/volume, HLB values, min projection area, and H-bond acceptor counts did not correlate with IFN-α expression. Factors with the strongest negative correlations with IFN-α expression included the LogS (intrinsic solubility, i.e., maximum solubility of the unionized species) and the H-bond donor sites of the lipids (**Figure 4B**). Higher H-bond donors and LogS are the most unfavorable features of these lipids for stimulating IFN-α. Since IFN-α is a pleiotropic cytokine that can be used to treat Multiple Sclerosis,[30] viral infections,[31] and cancer,[23, 32] preferential IFN-α stimulation by these novel lipids have the potential to further developed for treating various diseases.

Conclusions

Novel immune-modulating biomaterials are of increasing interest in the immunotherapy era. Immune-modulating lipids are an important class of biomaterial due to their versatilities in formulating various drug and gene delivery systems such as liposomes or nucleic acid delivery lipid nanoparticles (e.g., the mRNA-delivering COVID vaccine). Developing novel immune-modulating lipid scaffolds would enable the next generation of immunotherapy. In this study, we designed and synthesized several single-tailed heterocyclic carboxamide lipids, hypothesizing that these lipids would have immune-modulating features based on their structural similarity to lipids involved in ceremide and S1P signaling pathways, as well as recently reported heterocyclic ionizable lipids.[4, 10, 33]

We evaluated the biological effects of these heterocyclic carboxamide lipids in macrophages and dendritic cells. Notably, these lipids preferentially modulated only the macrophages but not the dendritic cells, mainly through interfering with sphingosine-1-phosphate lyase[18] and IFN-α expression.[11] Future studies could include single-cell sequencing studies to better understand the underlying mechanism of action between the differential modulation between macrophage and dendritic cells.

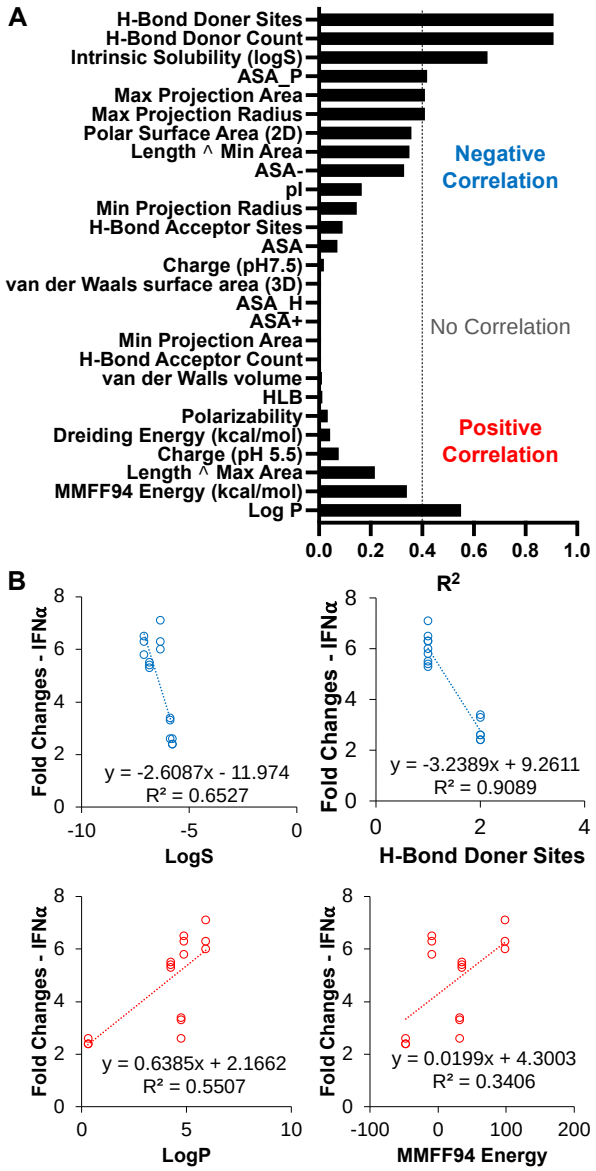

Figure 4. Correlation analysis of IFNα expression levels as a function of lipid physicochemical properties. A) Each physical property is ranked based on its R^2 values of correlation, then categorized as a positive or negative correlation based on the linear regression slope. B) Selective examples of factors that have the strongest negative (*e.g.,* LogS and H-Bond Doners) and positive (*e.g.,* LogP and MMFF94 energy) correlations to the expression levels of IFNα. The complete list of correlation data is shown in **Figure S24**.

Furthermore, our extensive correlation analysis identified key physicochemical properties positively and negatively associated with the observed immune modulation. These observations provide insights into the future development of cell-type-specific immune-modulating lipids. Furthermore, our heterocyclic carboxamide lipids have great potential to be further derivatized *via* their click-chemistry-enabling propargyl side chains. Heterocyclic carboxamide lipids are easy to make and purify, with preferential action in macrophages but not dendritic cells, providing promising features that pave the way for the future development of lipid-based immune engineering.

Although lipids are often administered in the form of liposomes or micelles, there are examples of lipids that do not require self-assembly to mediate therapeutic efficacy. For example, the

clinically approved S1PR modulator, Fingolimod, is given orally as tablets/capsules. Thus, self-assembly properties were not the top priorities when designing and testing these lipid-mimic molecules. While it was observed that not all KM lipids self-assemble into micelles at physiological pH, lipids **KM1** and **KM4** can be micellarized when ionized at lower pH. Additionally, all lipids exhibit excellent solubility in alcohols, making them promising candidates for co-formulation with liposomes or lipid nanoparticles via microfluidic systems. Furthermore, the hydroxyl groups of these lipids provide opportunities for esterification with fatty acids, enabling modular self-assembly properties. Given these properties, investigating the use of KM lipids as nano-formulations in future studies would be an intriguing area of research.

Acknowledgment

This work was partly funded by the NIH R21GM135853, R01HL161456, R01CA241679, the National Science Foundation DMR 2000256, the Eshelman Institute for Innovation, and the Research Foundation for the State University of New York at Binghamton faculty startup fund. Natalie Jasiewicz received funding from the PhRMA fellowship.

Conflicts of interest

"There are no conflicts to declare."

Notes and references

Details of chemical synthesis and purification, NMR spectra, ESI-MS spectra, PCR primer sequences, and PCA results are available online as supporting information.

1. *Nature Reviews Materials*, 2019, **4**, 349-349.
2. M. J. Hubler and A. J. Kennedy, *The Journal of Nutritional Biochemistry*, 2016, **34**, 1-7.
3. D. P. Vangasseri, Z. Cui, W. Chen, D. A. Hokey, L. D. Falo and L. Huang, *Molecular Membrane Biology*, 2006, **23**, 385-395.
4. C. J. Pritzl, Y.-J. Seo, C. Xia, M. Vijayan, Z. D. Stokes and B. Hahm, *The Journal of Immunology*, 2015, **194**, 4339-4349.
5. K.-C. Mei, Y.-P. Liao, J. Jiang, M. Chiang, M. Khazaieli, X. Liu, X. Wang, Q. Liu, C. H. Chang, X. Zhang, J. Li, Y. Ji, B. Melano, D. Telesca, T. Xia, H. Meng and A. E. Nel, *ACS Nano*, 2020, **14**, 13343-13366.
6. A. E. Nel, K.-C. Mei, Y.-P. Liao and X. Liu, *ACS Nano*, 2022, **16**, 5184-5232.
7. E. L. Etter, K.-C. Mei and J. Nguyen, *Advanced Drug Delivery Reviews*, 2021, **179**, 113994.
8. X. Hou, T. Zaks, R. Langer and Y. Dong, *Nature Reviews Materials*, 2021, **6**, 1078-1094.
9. L. Miao, L. Li, Y. Huang, D. Delcassian, J. Chahal, J. Han, Y. Shi, K. Sadtler, W. Gao, J. Lin, J. C. Doloff, R. Langer and D. G. Anderson, *Nature Biotechnology*, 2019, **37**, 1174-1185.
10. L. Kappos, E.-W. Radue, P. O'Connor, C. Polman, R. Hohlfeld, P. Calabresi, K. Selmaj, C. Agoropoulou, M. Leyk, L. Zhang-Auberson and P. Burtin, *New England Journal of Medicine*, 2010, **362**, 387-401.
11. M. Vijayan, C. Xia, Y. E. Song, H. Ngo, C. J. Studstill, K. Drews, T. E. Fox, M. C. Johnson, J. Hiscott, M. Kester, S. Alexander and B. Hahm, *The Journal of Immunology*, 2017, **199**, 677-687.
12. T. Kawai and S. Akira, *Trends in Molecular Medicine*, 2007, **13**, 460-469.
13. J. Chun, G. Giovannoni and S. F. Hunter, *Drugs*, 2021, **81**, 207-231.
14. A. Garcia-Diaz, D. S. Shin, B. H. Moreno, J. Saco, H. Escuin-Ordinas, G. A. Rodriguez, J. M. Zaretsky, L. Sun, W. Hugo, X. Wang, G. Parisi, C. P. Saus, D. Y. Torrejon, T. G. Graeber, B. Comin-Anduix, S. Hu-Lieskovan, R. Damoiseaux, R. S. Lo and A. Ribas, *Cell Reports*, 2017, **19**, 1189-1201.
15. D. Jorgovanovic, M. Song, L. Wang and Y. Zhang, *Biomarker Research*, 2020, **8**, 49.
16. P. Fitzgerald-Bocarsly and D. Feng, *Biochimie*, 2007, **89**, 843-855.
17. Q. Xue, Y. Yan, R. Zhang and H. Xiong, *International Journal of Molecular Sciences*, 2018, **19**, 3805.
18. M. Serra and J. D. Saba, *Advances in Enzyme Regulation*, 2010, **50**, 349-362.
19. A. M. Bryan and M. Del Poeta, *Cellular Microbiology*, 2018, **20**, e12836.
20. A. V. Bazhin, K. von Ahn, J. Fritz, J. Werner and S. Karakhanova, *Frontiers in Immunology*, 2018, **9**.
21. Y. Liu, X. Liang, X. Yin, J. Lv, K. Tang, J. Ma, T. Ji, H. Zhang, W. Dong, X. Jin, D. Chen, Y. Li, S. Zhang, H. Q. Xie, B. Zhao, T. Zhao, J. Lu, Z.-W. Hu, X. Cao, F. X.-F. Qin and B. Huang, *Nature Communications*, 2017, **8**, 15207.
22. K. Abiko, N. Matsumura, J. Hamanishi, N. Horikawa, R. Murakami, K. Yamaguchi, Y. Yoshioka, T. Baba, I. Konishi and M. Mandai, *British Journal of Cancer*, 2015, **112**, 1501-1509.
23. L. Zhang, Y.-T. Tai, M. Z. G. Ho, L. Qiu and K. C. Anderson, *Experimental Hematology & Oncology*, 2017, **6**, 20.
24. J.-H. Lai, L.-F. Hung, C.-Y. Huang, D.-W. Wu, C.-H. Wu and L.-J. Ho, *Arthritis Research & Therapy*, 2021, **23**, 120.
25. Y. Gui, H. Zheng and R. Y. Cao, *Frontiers in Cardiovascular Medicine*, 2022, **9**.
26. A. Skoura, J. Michaud, D.-S. Im, S. Thangada, Y. Xiong, J. D. Smith and T. Hla, *Arteriosclerosis, Thrombosis, and Vascular Biology*, 2011, **31**, 81-85.
27. X. Wang, S. Chen, H. Xiang, X. Wang, J. Xiao, S. Zhao, Z. Shu, J. Ouyang, Z. Liang, M. Deng, X. Chen, J. Zhang, H. Liu, Q. Quan, P. Gao, J. Fan, A. F. Chen and H. Lu, *Biochemical Pharmacology*, 2022, **201**, 115077.
28. T. Metsalu and J. Vilo, *Nucleic Acids Research*, 2015, **43**, W566-W570.
29. T. A. Halgren, *Journal of Computational Chemistry*, 1996, **17**, 490-519.
30. L. Durelli, M. R. Bongioanni, R. Cavallo, B. Ferrero, R. Ferri, E. Verdun, G. B. Bradac, A. Riva, M. Geuna, L. Bergamini and et al., *Mult Scler*, 1995, **1 Suppl 1**, S32-37.
31. C. E. Samuel, *Clin Microbiol Rev*, 2001, **14**, 778-809, table of contents.
32. M. Ferrantini, I. Capone and F. Belardelli, *Biochimie*, 2007, **89**, 884-893.
33. T. Nakamura, T. Sato, R. Endo, S. Sasaki, N. Takahashi, Y. Sato, M. Hyodo, Y. Hayakawa and H. Harashima, *Journal for ImmunoTherapy of Cancer*, 2021, **9**, e002852.